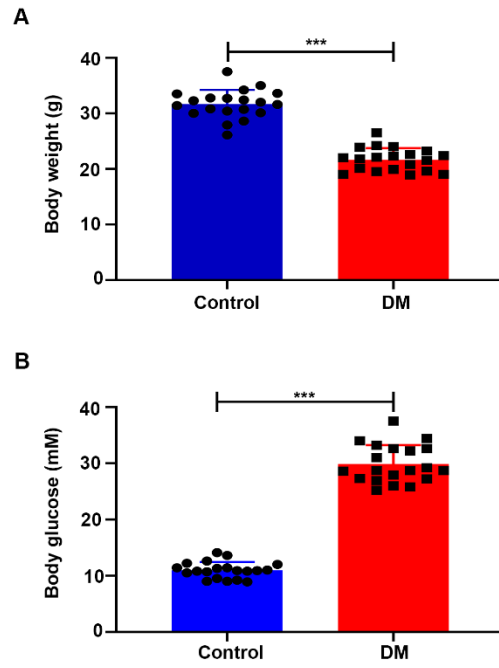


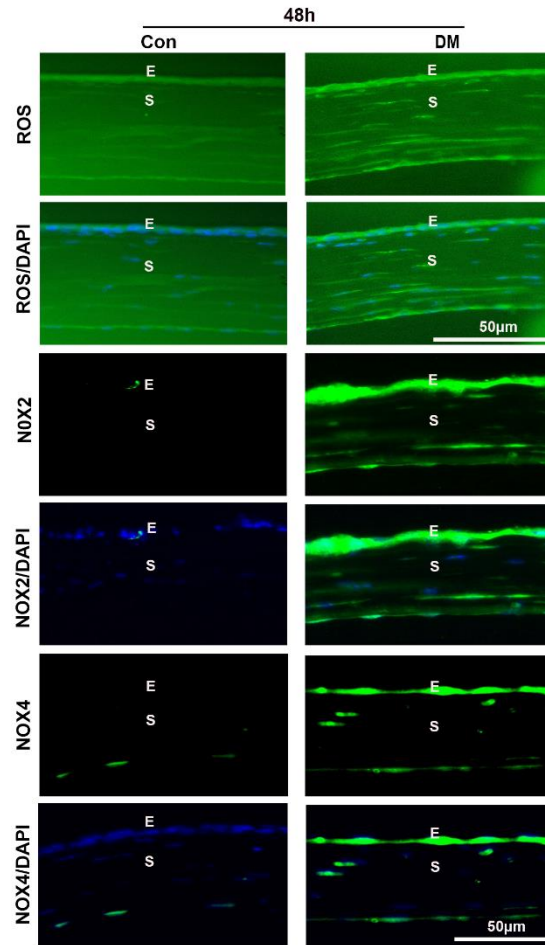
**Suppl.Table.1 Antibodies for western blotting, immunofluorescence and immunohistochemistry**

<b>Primary antibody</b>	<b>Dilution concentration</b>	<b>Supplier</b>	<b>Code</b>
Anti-ANLRP3	WB (1/1000) IF (1/200) IHC (1/200)	Cell Signaling Technology	15101
Anti- ASC	WB (1/1000)	Cell Signaling Technology	67824
Anti- Caspase-1	WB (1/1000)	Cell Signaling Technology	24232
Anti-IL-1 $\beta$	WB (1/1000) IHC (1/200)	Cell Signaling Technology	31202
Anti-IL-1 $\beta$	IF (1/200)	Abcam	ab9722
Anti- GSDMD	WB (1/1000) IF (1/200)	Abcam	ab209845
Anti-AGE	WB (1/1000) IF (1/200) IHC (1/100)	BIOSS	Bs-1158R
Anti-NADPH oxidase 2	WB (1/1000) IF (1/200)	Abcam	ab129068
Anti-NADPH oxidase 4	WB (1/1000) IF (1/200)	Abcam	ab133303
Anti-Ki67	IF (1/200)	Abcam	ab16667
Anti- $\beta$ -actin	WB (1/2000)	Cell Signaling Technology	4970
Anti-p-Stat3	IF (1/200)	Abcam	ab68153
anti -Tubulin Beta 3 (TUBB3)	IF (1/200)	Biologend	657403
Alexa Fluor 488 goat anti-rabbit IgG	IF (1/200)	Beyotime	A0423
Goat anti-rat IgG	WB (1/3000)	Proteintech	SA00001-2

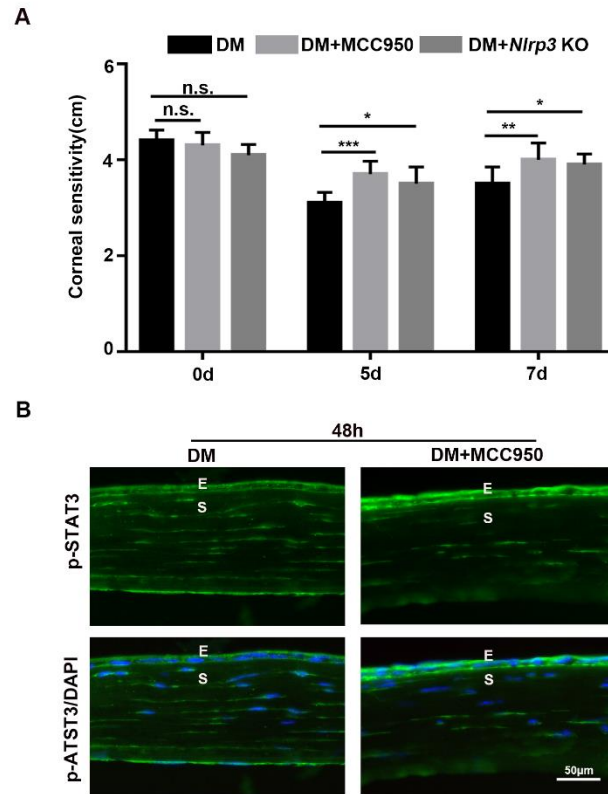
Abbreviations: WB, western blotting; IF, immunofluorescence; IHC, immunohistochemistry



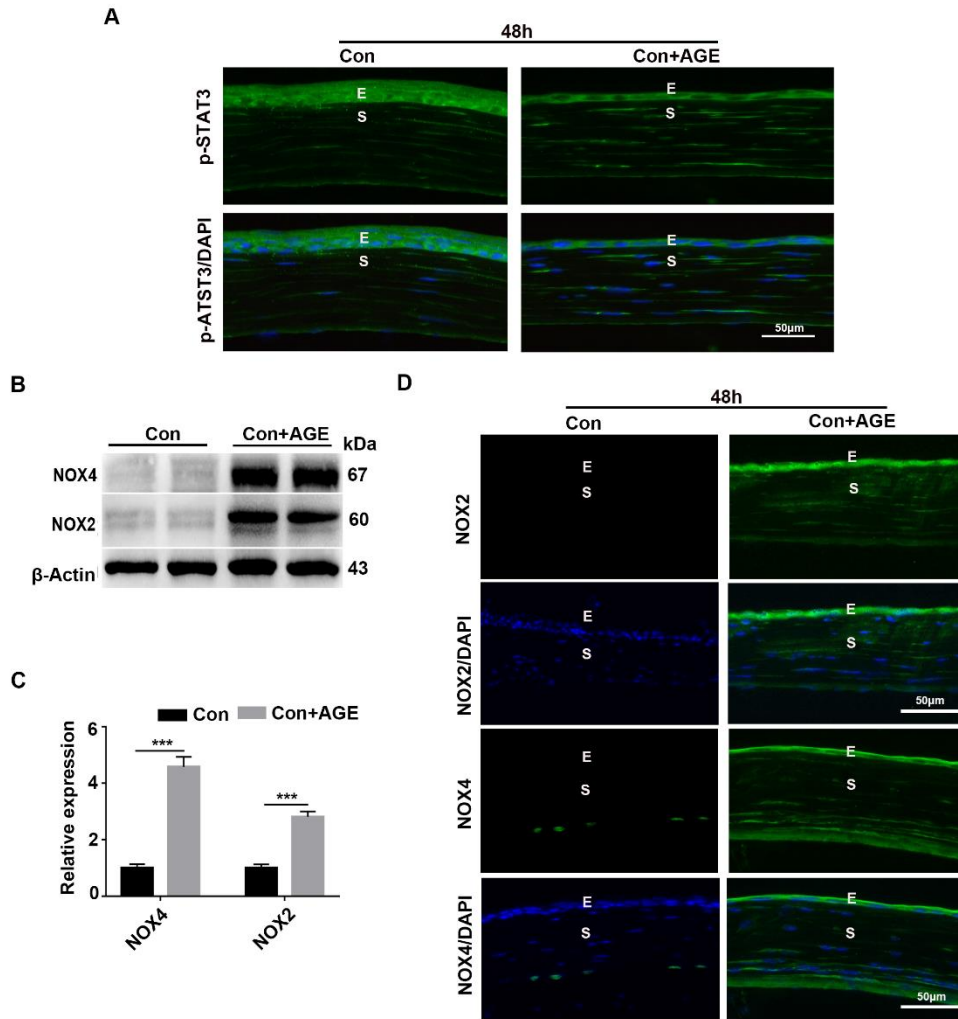
**Suppl. Fig. 1 Body weight and glucose of normal mice and type 1 diabetic mice.** (A) Body weight of normal and type 1 diabetic mice. (B) Blood glucose of normal and type 1 diabetic mice. (n = 20/group). \*\*\*P < 0.001.



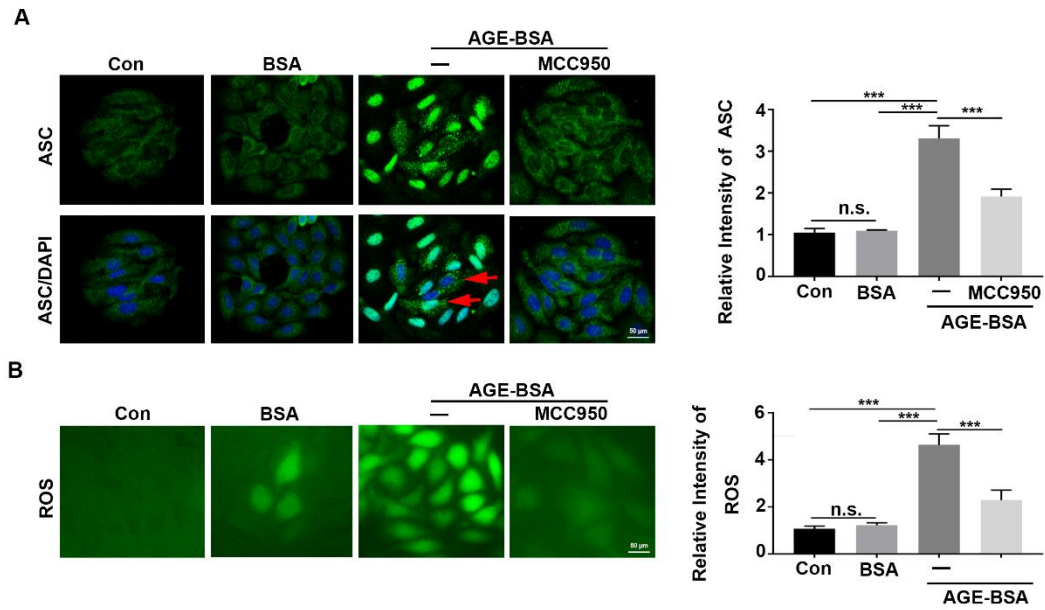
**Suppl. Fig. 2. The diabetic corneas displayed increased levels of ROS, NOX2 and NOX4 at 48h after corneal epithelial abrasion.** The levels of ROS, NOX2 and NOX4 in corneas at 48h after corneal epithelial abrasion were detected using immunofluorescence staining. E, epithelium; S, stroma.



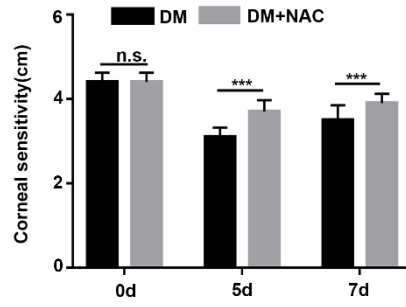
**Suppl. Fig. 3. Blocking NLRP3 inflammasome activation accelerated the corneal sensitivity recovery and increased signal transducer and activator of transcription 3 (STAT3) activity in diabetic mice.** (A) The corneal sensation at 5 and 7 d after corneal epithelial removal was tested by a Cochet-Bonnet esthesiometer (n=5). (B) The expression of p-STAT3 in the corneas at 48 h after epithelial injury was determined using immunofluorescence staining. E, epithelium; S, stroma. Data were showed as mean  $\pm$ SD. n.s, not significant, \* P <0.05, \*\* P <0.01, \*\*\* P <0.001.



**Suppl. Fig. 4. Exogenous AGEs promoted oxidative stress and inhibited STAT3 activation in normal mice.** (A) The activation of STAT3 in the cornea at 48 h after epithelial injury was determined by p-STAT3 staining (n=3). (B) The levels of NOX2 and NOX4 in AGE-treated corneas at 48h after epithelial abrasion were tested by western blot. (C) The relative expression of NOX2 and NOX4 as in (B) was quantified by Image J (n=3). (D) The expression of NOX2 and NOX4 in the corneas at 48 h after epithelial injury was examined using immunofluorescence staining (n=3). Data were presented as mean  $\pm$ SD. E, epithelium; S, stroma. Data were showed as mean  $\pm$ SD. \*\*\* P <0.001.



**Suppl. Fig. 5. AGEs promoted NLRP3 inflammasome activation and accumulation of ROS in TKE2 cells.** (A) The ASC in AGE-BSA-treated TKE2 in the presence or absence of MCC950 was evaluated by immunofluorescence staining (n=3). Left, the intensity of ASC in different groups was quantified by Image J software. The ASC foci were shown by red arrows. (B) The ROS accumulation in AGE-BSA-treated TKE2 in the presence or absence of MCC950 was evaluated by DCFH-DA. Left, the intensity of ROS in different groups was determined by Image J software. Data were showed as mean  $\pm$ SD. n.s, not significant, \*\*\* P <0.001.



**Suppl. Fig. 6. NAC accelerated the corneal sensitivity recovery in diabetic mice.** The corneal sensation was tested by a Cochet-Bonnet esthesiometer at 5 and 7 d after epithelial removal in the diabetic mice treated or untreated with NAC (n=5). Data were given as mean  $\pm$ SD, n.s, not significant, \*\*\* P <0.001.